High Voltage, High Hopes: A Cautionary Tale of Through-Thickness Electroplastic for Springback Reduction

Eneko Saenz de Argandoña
Mondragon Unibertsitatea
Manex Barrenetxea
Mondragon Unibertsitatea
Iosu Aizpuru
Mondragon Unibertsitatea
Javier Trinidad
Mondragon Unibertsitatea
Nagore Otegi
Mondragon Unibertsitatea
Joseba Mendiguren
jmendiguren@mondragon.edu

Mondragon Unibertsitatea

Research Article

Keywords: electroplasticity, springback, SDG, Sheet metal forming, Springback reduction, Pulse forming, Process failure, Sustainable manufacturing

Posted Date: November 3rd, 2025

DOI: https://doi.org/10.21203/rs.3.rs-7242556/v2

Additional Declarations: The authors declare no competing interests.

High Voltage, High Hopes: A Cautionary Tale of Through-Thickness Electroplastic for Springback Reduction

Eneko Saenz de Argandoña[a], Manex Barrenetxea[a], Iosu Aizpuru[b], Javier Trinidad[a], Nagore Otegi[a], Joseba Mendiguren [a,1]

[a]*Mondragon Unibertsitatea, Faculty of Engineering, Mechanics and Industrial Production Department, Mondragon, Spain*

[b]*Mondragon Unibertsitatea, Faculty of Engineering, Electronics and Computer Science Department, Mondragon, Spain*

https://doi.org/10.21203/rs.3.rs-7242556/v1

Abstract

This work explores the feasibility of inducing springback reduction in AA5754 aluminium alloy sheets using a novel approach: Post-Forming Through-Thickness Electroplastic Effect (PF-TT-EPE). The concept aims to deliver high-energy electrical pulses directly through the sheet thickness via embedded tooling electrodes, enabling stress relaxation without external fixtures or process interruption. While theoretically promising, the experimental campaign encountered critical implementation challenges. Despite establishing a repeatable baseline springback of 11.8±0.5°, all attempts to apply pulse trains above ~600 A·ms/mm² resulted in uncontrolled spark discharge, severe sample damage, and tooling degradation, linked to air gap formation and dielectric breakdown at the interface. At lower energies, the process proved electrically safe but ineffective in reducing springback. These findings highlight the fragility of die-integrated electrical delivery systems and expose the hidden complexity of ensuring stable, conductive contact under forming conditions. Rather than demonstrating success, this study contributes a clear boundary to the applicability of electroplastic forming techniques and outlines the key technical gaps that must be closed for PF-TT-EPE to move beyond concept.

Keywords: *electroplasticity, springback, SDG, Sheet metal forming, Springback reduction, Pulse forming, Process failure, Sustainable manufacturing*

[1] Corresponding author.

E-mail address: jmendiguren@mondragon.edu (J.Mendiguren)

1. Introduction

Stamping is a cornerstone of mass production in the manufacturing of lightweight components, particularly in the automotive and aerospace sectors [1]. However, elastic recovery, commonly known as springback, remains a persistent challenge, often resulting in dimensional inaccuracies, increased reworking time, and even part rejection [2], [3], [4], [5]. These issues are exacerbated in high-strength alloys and complex geometries, where elastic recovery becomes difficult to predict and control. The implications are not limited to the forming process itself; rather, they cascade throughout the entire manufacturing chain, affecting die design, trimming strategies, and assembly precision [6], [7], [8]. From the perspective of sustainable manufacturing and the United Nations Sustainable Development Goals (SDGs), minimizing material waste and improving process efficiency are critical [9].

This has driven the exploration of alternative techniques to mitigate springback, including the use of stress-relief treatments and advanced forming technologies [10], [11], [12]. One such emerging approach is the Electroplastic Effect (EPE) [13], [14], [15], which has shown promise in altering the mechanical response of metals under electric current [16]. Yet, implementing EPE in industrial settings remains complex and challenging compared to more conventional stress-relaxation methods, such as thermal treatments. A key question arises: Can stress relaxation be effectively induced through a high-energy electrical pulse applied immediately after forming in that millisecond while the forming tools are still closed? If achievable, this would enable the application of targeted current pulses through the sheet thickness, leveraging the intimate contact between die and material, to reduce or even eliminate springback [17]. Such a breakthrough could unlock new possibilities in forming extreme geometries while contributing meaningfully to sustainable production goals [18].

Recent studies have explored the potential of using post-forming electrical pulses to induce stress relaxation without compromising material integrity. In earlier work, it was demonstrated that applying a train of low to moderate energy electrical pulses after plastic deformation could significantly reduce internal stresses in AA5754 aluminium alloy without causing recrystallization or degradation of mechanical properties [16]. This phenomenon, referred to as the Post-Forming Electroplastic Effect (PFEPE), was further investigated in subsequent research, where it was shown to effectively reduce springback in V-bending operations through post forming current application [17]. These findings confirmed that electrical pulses, when carefully controlled, can alter the dislocation structure and promote grain boundary rearrangement, offering a non-thermal route to stress relief.

However, these experiments relied on current flow along the surface of the specimen, which limits industrial applicability due to the need for external contact electrodes and precise alignment. A possible next step would be to explore whether similar stress-relief effects can be achieved by passing current directly through the sheet thickness, leveraging the mechanical and electrical interface already present between the sheet and forming tools during industrial operations.

In this context, the present work investigates the feasibility of applying high-energy electrical pulse trains through the thickness of a metal sheet immediately after forming, using the forming tools themselves as current electrodes, a process referred to here as the **Post-Forming Through-Thickness**

Electroplastic Effect (PF-TT-EPE). This concept aims to simplify implementation by integrating stress-relaxation treatment directly into existing industrial tooling, thereby avoiding additional process steps or external contact systems. If successful, PF-TT-EPE could enable in-die springback compensation, expanding the range of achievable geometries while supporting energy-efficient and sustainable manufacturing practices. To test this hypothesis, a novel V-bending tool was developed with insulated electrical connections embedded into both upper and lower dies, allowing current to flow directly through the sheet thickness. Despite promising theoretical foundations, the experimental campaign revealed unexpected failure mechanisms, such as spark discharge and material degradation at the contact interface, which highlight the challenges of translating electroplastic concepts into practical forming operations. This paper presents the motivation, methodology, and lessons learned from this failed attempt, contributing to the growing body of knowledge on electrically assisted forming and supporting more realistic paths toward industrial integration.

2. Background and Related Work

Recent efforts to reduce springback in metallic sheet forming have explored the application of pulsed electrical current as a means to induce stress relaxation post-deformation. In tensile stress-relaxation tests on AA5754 aluminium alloy, a clear force drop was observed when electrical pulse trains were applied under constant strain conditions. These findings confirmed that pulses with energy densities below ~4000 A·ms/mm² could significantly reduce internal stresses without degrading mechanical properties, primarily through dislocation rearrangement and electron-dislocation interaction mechanisms [16]. Figure 1 illustrates the experimental setup and representative force–time curves from these tests.

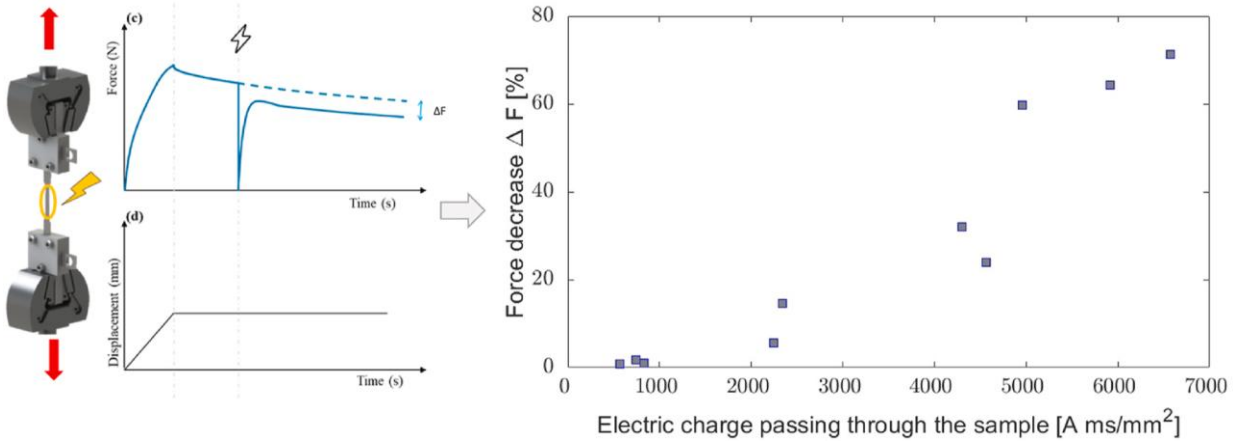

Figure 1. Experimental results from previous work on stress-relaxation tests, [16]. The left side illustrates the experimental setup, where a tensile test specimen is held between two non-conductive grips. The right side presents the observed force reduction following the application of a train of electrical pulses during a constant strain holding phase.

This concept was extended to V-bending operations to evaluate springback response under more realistic forming conditions. As shown in Figure 2, a post-forming electrical pulse train with energy

as low as ~800 A·ms/mm² produced a sharp drop in springback angle, while higher charge levels yielded diminishing additional benefit [17].

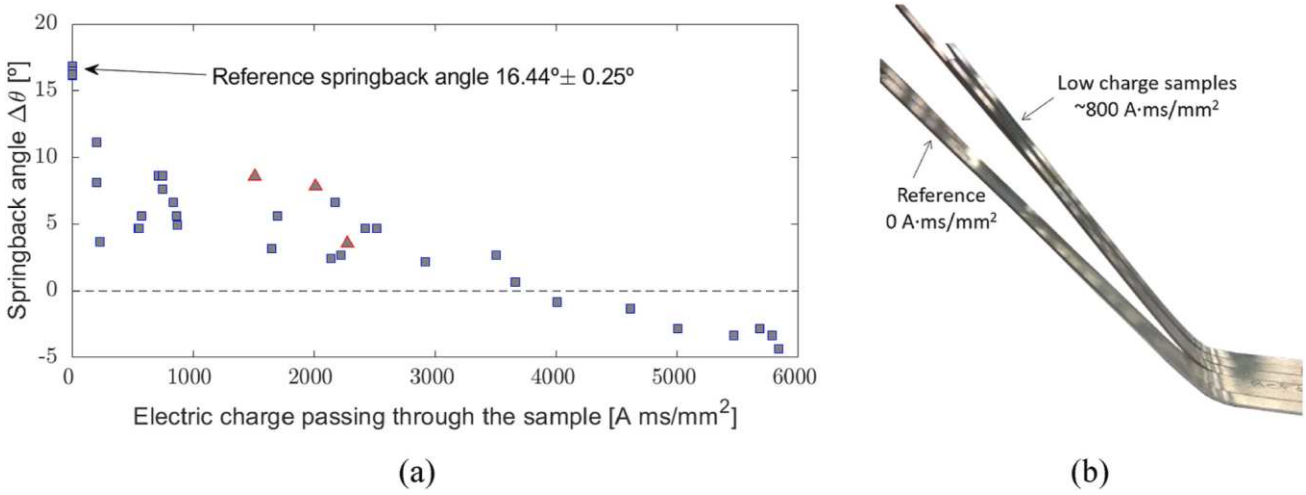

Figure 2. Experimental results from previous work on V-bending springback reduction tests, [17]. The left side illustrates the evolution of the springback angle as a function of the effective energy of the applied pulse train (at room temperature, squares, and cryogenic conditions, triangles), while the right side highlights the springback reduction achieved by comparing the reference condition (0 A·ms/mm²) to the result after applying a pulse train with an effective energy of approximately 800 A·ms/mm².

This abrupt change, not mirrored in the tensile force-relaxation data, indicates that different mechanisms, or at least different sensitivities, govern springback and tensile recovery responses under electrical stimulation. Finite element simulations and analytical modelling conducted in the same study identified the skin-effect as a potential key factor in this discrepancy: current density was shown to concentrate near the surface of the sheet due to the high-frequency nature of the pulses, aligning with regions of highest plastic strain in bending. This surface-localized current could selectively relieve residual stresses critical to springback, while having limited influence on bulk tensile behaviour. Nevertheless, numerical study performed at [17], did not show strong evidence supporting this hypothesis and therefore this still remains unanswered.

To capture this decoupling between force relaxation and geometric recovery, Table 1 summarized the effects of three energy levels (low, medium, and high) on both metrics [17]. Most strikingly, low-energy pulses that produced less than 5% force reduction in the tensile tests resulted in a springback reduction of 40–60%, highlighting a possible *shock-like or transient electromechanical effect* that is yet to be fully understood. This nonlinear trend persisted across the charge spectrum: both low–medium and medium–high energy levels were effective in reducing springback, but only moderately altered force response. These results reinforce the idea that springback and stress-relaxation mechanisms under pulsed current may not be governed by identical microphysical processes.

Table 1. Summary of the impact of different electric charges in force reduction (second raw) and springback angle reduction [17].

	Low charges	Low-medium charges	Medium-high charges	High charges
	<1000 A·ms/mm²	2000-3000 A·ms/mm²	3000-5000 A·ms/mm²	>5000 A·ms/mm²
ΔF	<5%	5-15%	25-35%	>50%
$\Delta\theta$	~40-60%	~50-80%	~70-100%	-

At the microstructural level, early interpretations attributed the observed stress-relief effects to dislocation rearrangement and annihilation mechanisms. EBSD and TEM studies revealed a transition from dislocation tangles to organized subgrain structures following pulsing, particularly in zones of high strain concentration. As summarized in Figure 3, and building on the classic framework by Humphreys and Hatherly [19], the process can be understood as follows: (a–c) Dislocation tangles evolve into cell structures via rearrangement and annihilation; (d) Dislocation networks dissolve through glide and climb mechanisms, enabled by localized energy input; (e–g) Elastic strain is converted into plastic strain via atom-scale activation, potentially assisted by electron wind effects.

This framework complements the previously mentioned observations: pulses below ~4000 A·ms/mm² can activate these mechanisms effectively, while exceeding ~5000 A·ms/mm² risks triggering localized recrystallization, particularly near current entry points.

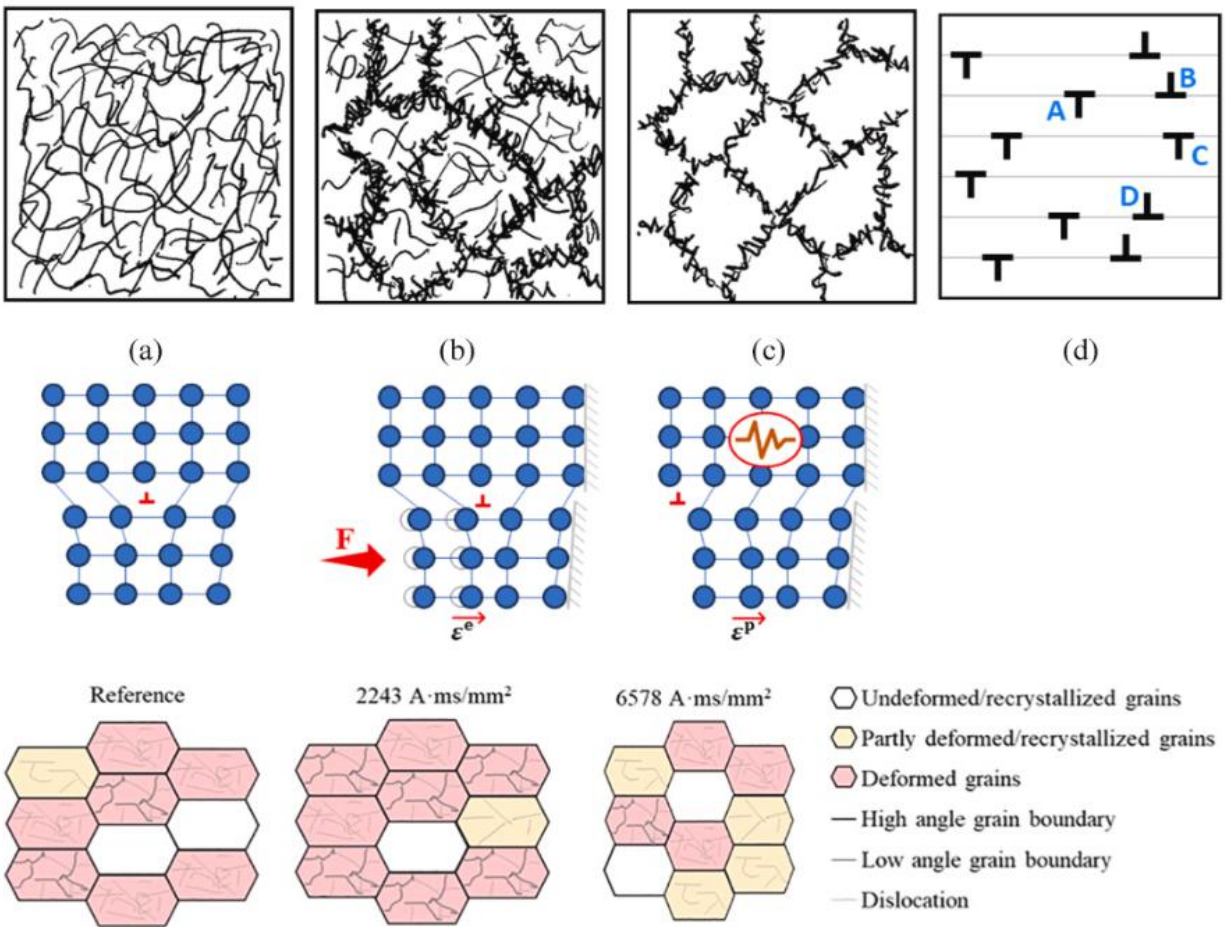

Figure 3. Combined representation of the microstructural mechanisms underlying stress relaxation induced by electrical pulses. Top: Internal stress reduction through dislocation rearrangement and atomic-scale mechanisms, [17]. Evolution from dislocation tangles to cell structures via rearrangement and annihilation. Dislocation annihilation by glide and climb mechanisms. Conversion of elastic strain to plastic strain through atomic vibration, potentially assisted by electron wind effects. Bottom: Schematic representation of the Post-Forming Electroplastic Effect (PFEPE), adapted from [16]. Low-energy pulses (<4000 A·ms/mm²) restructure low-angle grain boundaries and dislocation networks, promoting stress relief without altering grain morphology. High-energy pulses (>5000 A·ms/mm²), however, can induce localized recrystallization, particularly near current entry and exit points.

Despite these promising insights, existing implementations relied exclusively on current paths along the surface of the material, requiring external electrodes and precise contact conditions. This configuration poses significant scalability issues for high-volume stamping operations. Moreover, surface-localized current, while effective for relieving near-surface stresses, may not fully address through-thickness residual stress profiles, especially in thicker or multi-layered sheets.

To overcome these limitations, the present study explores the feasibility of the **Post-Forming Through-Thickness Electroplastic Effect (PF-TT-EPE)**: a process in which current is passed through thickness electrically connected forming dies. Basically, in one side of the sheet is one die with one electric connector, on the other side is the other die with the other electric connector, and this

makes the electricity to pass through the thickness of the sample in a localised manner. This approach aims to activate stress-relaxation mechanisms more uniformly across the material cross-section, without requiring process interruption or additional tooling. As will be shown, the transition from concept to practice revealed several physical and electrical limitations, including spark formation and contact instability, that must be addressed before PF-TT-EPE can be applied in industrial settings.

3. Experimental Setup

3.1. Material

The material used in this study was a 0.8 mm thick AA5754-H22 aluminium alloy sheet, identical batch to that used in previous investigations [16], [17]. This alloy is widely adopted in automotive structural components due to its good formability and corrosion resistance. The rolling direction (RD) was clearly marked and aligned with the bending direction in all tests. Prior microstructural characterization performed in earlier studies [16] confirmed the presence of elongated grains oriented along the RD, with moderate anisotropy and a weak texture typical of strain-hardened aluminium alloys. The initial grain size ranged between 25 and 40 µm, with a heterogeneous distribution of low-angle and high-angle grain boundaries. This microstructural baseline is relevant for interpreting the electroplastic response, as dislocation density and grain orientation influence the mobility of dislocations under pulsed current.

3.2. Pulse train generator

The electrical pulse train was delivered using a custom-built, ad hoc generator system previously developed and validated in earlier works. As illustrated in Figure 4, the system consists of a charging unit, a high-capacity capacitor bank, a set of thyristors for pulse timing control, and a discharge circuit capable of delivering high-current pulses with precise control of energy input. The capacitors operate at direct-current DC voltages ranging from 0 V to 540 V. Discharge times and pulse durations can be adjusted between 50 µs and 2 ms, enabling the generation of current densities in the range of 500 to 8000 A·ms/mm², depending on the capacitor DC voltage, contact resistance and discharge path. All pulses in this study were applied as a single burst or as a sequence of controlled pulses (pulse train). The system was manually operated and equipped with safety cutoffs to prevent accidental overcharging or discharge faults.

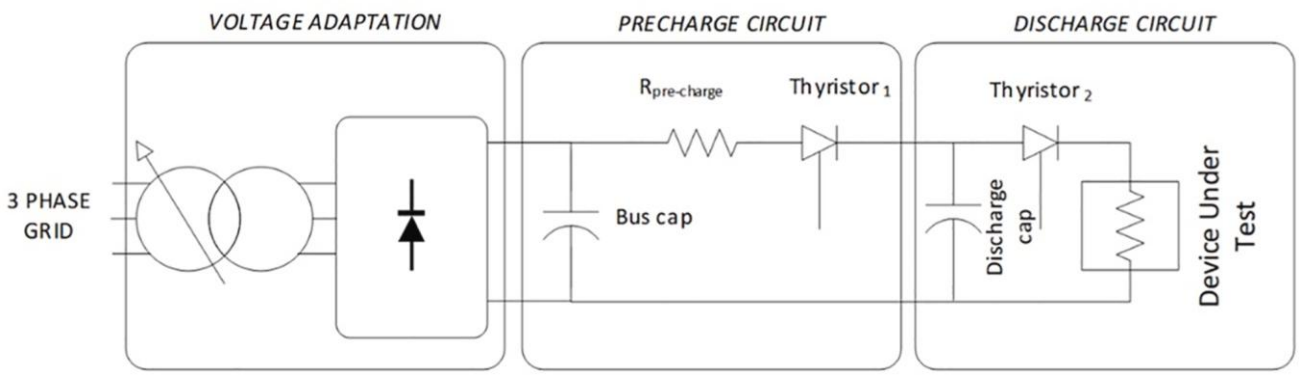

Figure 4. AD hoc pulse train generator architecture, [16].

3.3. PF-TT-EPE V-bending device

The experimental V-bending tool was specifically designed to explore the feasibility of applying post-forming electrical pulses through the sheet thickness, using the forming tools as electrodes. The bedding angle was of 90º and punch radius of 10 mm and a die radius of 10.8 mm to allocate the material thickness. The system, shown in Figure 5, consists of upper and lower steel dies with embedded electrical contacts located at the die radius. Each die is equipped with 5 electrical contacts, each 2 mm in diameter, uniformly spaced at 10 mm intervals. Both dies were constructed using RAKU®TOOL WB-1250 as high resistance electrically insulated material in order to insulate from the press base. The electrical terminals were connected to the pulse generator via high-current flexible cables, allowing for direct current flow across the sheet thickness when the dies were closed.

Figure 5a shows the full setup, including connection cables and die assembly; Figure 5b presents a close-up of the lower die with visible connection ports inside the cavity radius; Figure 5c shows the upper die, where the counterpart electrode connections are also embedded in the die radius. This configuration was designed to localize the current path to the region of highest bending strain, thus maximizing the potential for springback mitigation through in-situ stress relaxation.

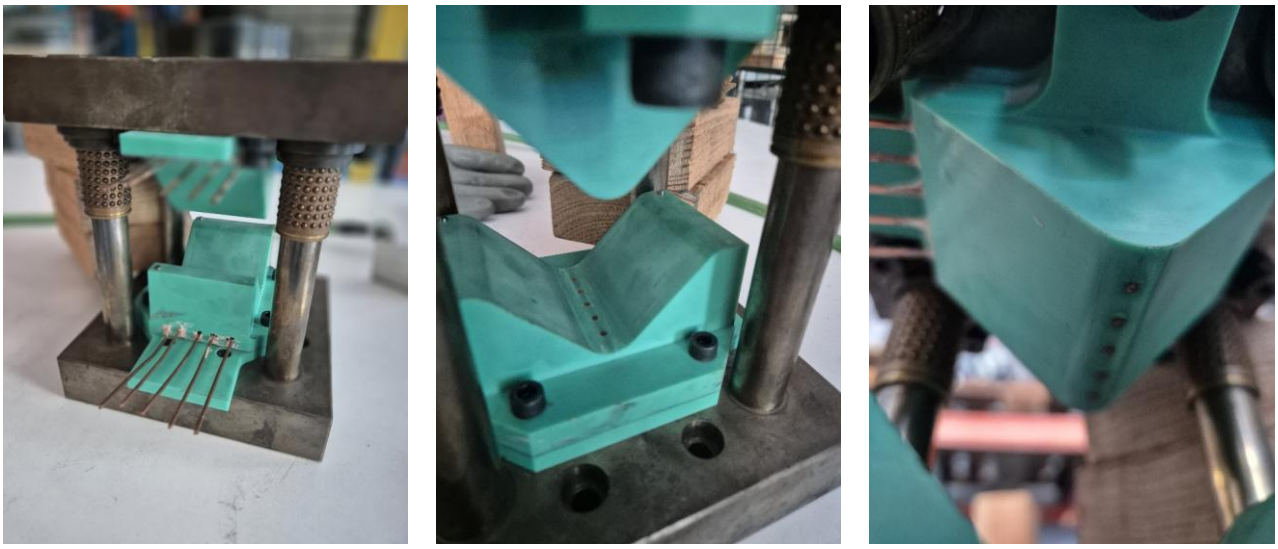

(a) (b) (c)

Figure 5. Experimental setup of the V-bending Post-Forming Through-Thickness Electroplastic Effect (PF-TT-EPE) device. The image shows: a) an overall view of the system, including both the upper and lower dies as well as the electrical connection cables; b) a close-up of the lower die, where the electrical connection points are integrated into the die radius cavity; and c) a close-up of the upper die, where the corresponding connection points are also visible along the die radius.

3.4. PF-TT-EPE V-bending testing methodology

The PF-TT-EPE forming trials were conducted under simplified conditions to reduce the risk of equipment damage in case of discharge failure. The procedure followed these sequential steps:

1. **Die opening**: The V-bending tool was opened to allow sample placement.
2. **Strip positioning**: AA5754 specimens (dimensions 50 mm × 100 mm) were inserted into the die cavity, with the rolling direction (RD) aligned parallel to the bend axis.
3. **Die closure:** The dies were closed manually, and external weights were applied to simulate die pressure without using a hydraulic press, minimizing the risk to laboratory equipment.
4. **Electrical cable connection:** The pulse generator terminals were connected to the designated upper and lower die electrodes using high-current leads.
5. **Pulse delivery:** The generator was triggered to discharge a single pulse train across the sample thickness.
6. **System shutdown:** After pulse delivery, the system was powered down, and capacitors were allowed to fully discharge to ensure safe handling.
7. **Tool opening:** The dies were manually opened, and the sample was carefully extracted.

Figure 6 shows representative figures of each step for the process. Each test was documented, and sample damage or electrical anomalies (such as sparking or arc traces) were noted. The full range of pulse energies tested, along with corresponding springback results and post-test observations, are presented in the next section.

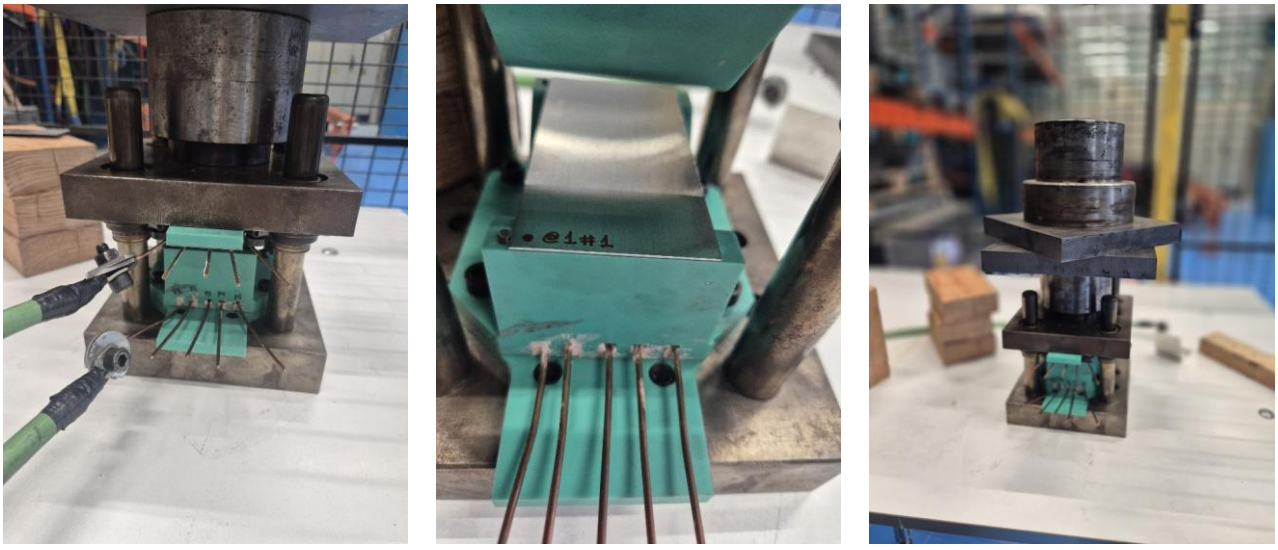

(a) (b) (c)

Figure 6. Experimental setup of the PF-TT-EPE device. The image shows: a) the pulse generator cables connected to deliver the electrical pulse train in the first contact point. b) a pair of pins in the lower die flat surface allowed the exact location of the sample prior to the test, and c) external weights were applied to simulate die pressure without using a hydraulic press, minimizing the risk to laboratory equipment.

It must be noted that the prototype testing die set was prepared with five different connector points, leading to five connectors on the top die and five on the bottom die that are arranged by pairs top to bottom (Fig. 6b or Fig.5a as example). To make the electricity to pass through one of the points (let's assume the first one for example), the pulse generator terminals need to be connected to the corresponding top and bottom connectors. As example Fig.6a shows the pulse generator cables connected to the first point's connectors; one to the top and the other one to the bottom to close the circuit. Therefore, in this prototype, if a pulse wants to be passed through the five points of the sample, methodology 4 to 6 needs to be repeated moving the cables from one spot to the next one. This means that the electric pulse is not given at the 5 points at the same time and these are given sequentially. This also allows to deliver different energy pulses to each point if needed.

3.5. V-bending springback calculations

The springback angle was estimated analytically based on geometric reconstruction of the deformed sample, using only one measurable parameter: the final width of the part after unloading. This indirect method relies on symmetry, conservation of length, and trigonometric projection. Figure 7 shows the schematic representation of the geometrical reconstruction of the bended sample.

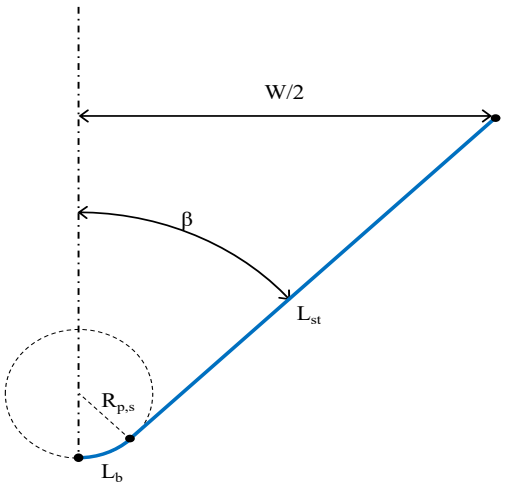

Figure 7. Schematic representation of the geometrical reconstruction of the bended sample. In the bended area the representative radiuses are presented, punch radius, R_p, and after springback radius, R_s, as well as the length of the arch, L_b. In the straight area, the length of the section, L_{st}, and the angle. This angle is 45º during forming and β after springback.

Each specimen had a total length of 100 mm. During forming, the sample was bent into a 90° V-shape over a punch with radius R_p = 10 mm. Assuming symmetry, only half the sample was analysed. This half consists of:

- A **bent region** with angle 45º and arc length:

$$L_b = \pi/4 \cdot R_p, \quad (1)$$

- A **straight region** of remaining length:

$$L_{st} = 100/2 - L_b. \quad (2)$$

After unloading, the geometry elastically opens due to springback. Two key changes occur:

1. The **bending radius increases** from R_p to $R_s > R_p$,
2. The **straight leg angle increases** from 45º to $\beta > 45º$, so the bent region reduces its angle as (90º-β).

The **projected width** of the half-sample (W/2) is composed of:

- The projection of the straight segment:

$$W_{st} = \sin(\beta)\, L_{st}. \quad (3)$$

- The projection of the bent arc segment:

$$W_b = \sin(\beta)\, R_s. \quad (4)$$

Since the arc length remains constant, it must satisfy:

$$L_b = R_s\, (\pi/2 - \beta), \quad (5)$$

And therefore:

$$W_b = \sin(\beta)\, L_b / (\pi/2 - \beta) \quad (6)$$

Then the total half-width becomes:

$$W/2 = \sin(\beta)\, L_b / (\pi/2 - \beta) + \sin(\beta)\, L_{st}. \quad (7)$$

This equation can be solved numerically for β given the measured width W, using the known values. Once β is calculated, the total opening angle of the bent part is 2β, and the springback deviation is:

$$\Delta\theta = 2\beta - 90^{o}. \quad (8)$$

All W measurements were taken using a calibrated digital calliper (±0.01 mm). This method avoids assumptions of fixed arc curvature and accounts for the redistribution of angular deformation during elastic recovery.

4. Experimental Campaign and Observations

The experimental campaign was designed to validate the feasibility of inducing springback reduction via through-thickness electrical pulse application using the PF-TT-EPE setup. The initial objective was to establish a baseline response and gradually increase pulse energy to evaluate the resulting effects on the geometry and material integrity of the formed part.

4.1. Baseline and Repeatability Assessment

To begin, five V-bending repetitions were performed under purely mechanical conditions, without any electrical input, to establish a baseline springback value. The average final bend angle across these trials was 101.8±0.5°, corresponding to a springback of 11.8±0.5° relative to the nominal 90° bend. The process was highly repeatable, with negligible variation between specimens, and within the measurement system accuracy. This springback angle differs from previous work [17], as previous work bending conditions were different from the current ones.

To confirm that the springback was independent of applied clamping force under the current conditions, an additional set of tests was conducted using a 40% increase in die clamping weight. The resulting springback angle remained unchanged at 101.8±0.5°, validating that the elastic recovery was not sensitive to moderate changes in normal pressure at die closure.

4.2. Initial Electrical Parameters and Scaling

Informed by previous studies, a pulse energy density of 3000 A·ms/mm² was selected as the initial target for pulse delivery. This level was previously shown to produce significant stress relaxation and springback reduction without inducing recrystallization or microstructural damage in AA5754 alloy [16], [17].

However, a key difference in the present setup was the geometry and area of the electric path. In earlier experiments, the current passed through compact tensile specimens with a cross-section of approximately 2 mm² (0.8 mm × 2.5 mm). In contrast, the embedded electrode contacts used in the current study had a diameter of 2 mm, resulting in a circular contact area of:

$$A = \pi\,(1\ \text{mm})^2 \sim 3.14\ \text{mm}^2. \quad (9)$$

To achieve an equivalent current density, the total pulse energy had to be scaled proportionally. This required increasing the delivered energy by a factor of 3.14 / 2 ≈ 1.57 to maintain similar energy per unit area.

4.3. Electrical Contact Challenges and Catastrophic Failure

The first trial conducted at this scaled-up energy level proved unsuccessful. Although mechanical contact between die and sample was apparently to be uniform and stable, the electrical contact proved unreliable. Suspecting inadequate conductivity at the interface, a premium carbon-based conductive grease (MG Chemicals™ 848) was applied to the contact zones between the sheet and the embedded electrodes.

Upon the next pulse delivery, the system experienced a violent spark discharge, accompanied by a loud thunder-like noise. Post-test inspection revealed a melted hole through the sheet at the contact region (see Figure 8), as well as severe electrode damage, including melting of the copper insert and localized degradation of the insulating resin at the die surface. This outcome indicated an extreme current localization and dielectric breakdown, confirming that the interface failed to conduct current uniformly.

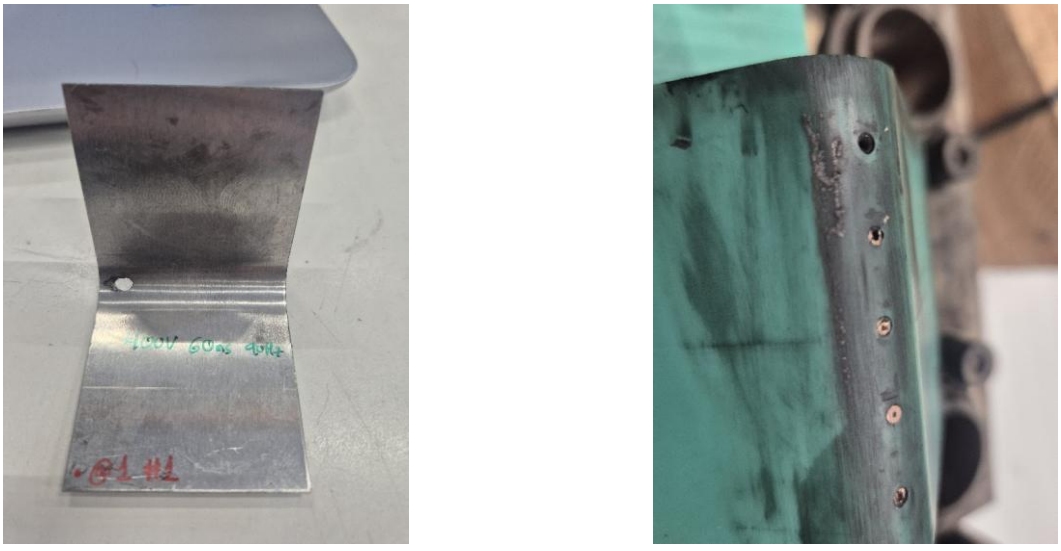

(a) (b)

Figure 8. Evidence of catastrophic failure following pulse delivery at 3000 A·ms/mm². (a) Melted hole observed in the sheet at the electrode contact point, caused by localized spark discharge. (b) Severe damage to the embedded tooling electrode, including melting of the copper insert and degradation of the surrounding insulating resin on the die surface.

4.4. Reduced Energy Testing and Re-Escalation

To avoid further equipment damage, the pulse energy was drastically reduced to a minimum of 274 A·ms/mm², well below previously studied effective thresholds. At this energy level, no spark

discharges or audible events were detected. However, the resulting springback angle remained identical to the baseline value of 101.8±0.5°, indicating no measurable effect of the electrical pulse at this level.

Subsequent tests increased the energy incrementally. At around 600 A·ms/mm², spark discharge and acoustic breakdown phenomena reappeared. To investigate whether voltage or frequency modulation could mitigate this behaviour, a pulse train with lower voltage (200 V) but extended pulse duration was attempted, maintaining equivalent energy delivery. However, the outcome was similarly destructive: severe melting, multiple perforations in the sample (see Figure 9), and further electrode degradation.

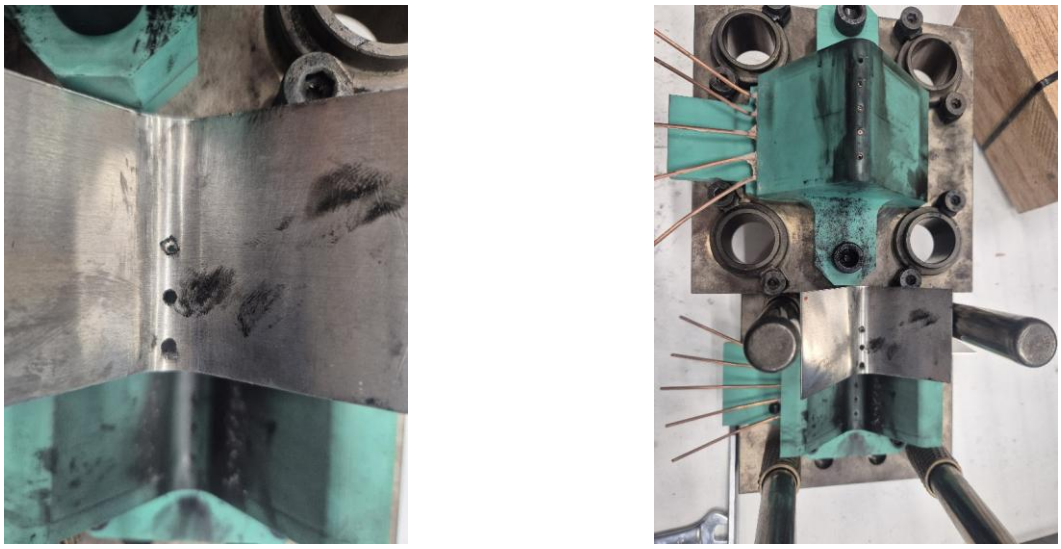

(a) (b)

Figure 9. Sample and tooling damage observed during the additional PF-TT-EPE trials with progressively increased pulse energy. (a) Formed sheet showing results of multiple pulse deliveries: initial low-energy pulses (< 300 A·ms/mm²) produced no visible damage but also no springback reduction, indicating insufficient interaction with the dislocation network. As the energy approached ~600 A·ms/mm², spark discharge and localized melting reappeared, resulting in visible perforations in the material. (b) Corresponding damage to the V-bending tooling, showing electrode destruction and severe surface degradation of the resin-insulated die due to repeated electrical breakdown.

These results indicate that despite theoretical energy alignment with previous EPE benchmarks, the through-thickness delivery mode using embedded tooling electrodes introduces critical challenges in electrical contact stability, current localization, and energy dissipation. Attempts to reproduce springback reduction under these conditions led to irreversible sample and tool damage (Fig. 8b and Fig. 9b), making the PF-TT-EPE approach, at least in its current form, unviable for reliable springback control.

5. Discussion

The results of the PF-TT-EPE campaign clearly demonstrate that, while the concept of applying electrical pulses through the thickness of a formed sheet is theoretically sound, its practical implementation introduces a number of critical challenges, most notably, the instability of the electrical interface between the tooling and the workpiece.

The observed spark discharges, often accompanied by thunder-like acoustic emissions and localized melting, are indicative of dielectric breakdown in air gaps formed unintentionally between the sample and the electrode surfaces [20]. Despite achieving what appeared to be full mechanical contact during die closure, it is likely that microscale surface irregularities, combined with uneven pressure distribution and oxide layers, resulted in localized non-contact zones. In these regions, the applied voltage can exceed the dielectric strength of air (approximately 3 kV/mm) [21], [22], causing electrical arcing across the gap. This is consistent with classical breakdown theory and previous observations in spot welding, micro-EDM, and pulsed current forming setups where electrical discharge phenomena are reported under similar contact conditions [23], [24].

A schematic representation of this phenomenon is shown in Figure 10, where the presence of a small air gap between the die and the sheet enables uncontrolled spark discharge upon pulse activation. The sudden discharge concentrates energy in a confined region, leading to rapid melting of both the sheet and the embedded electrode, as seen in Figures 8 and 9. This mechanism not only compromises the integrity of the part but also severely damages the tooling, making the process unsustainable in its current form.

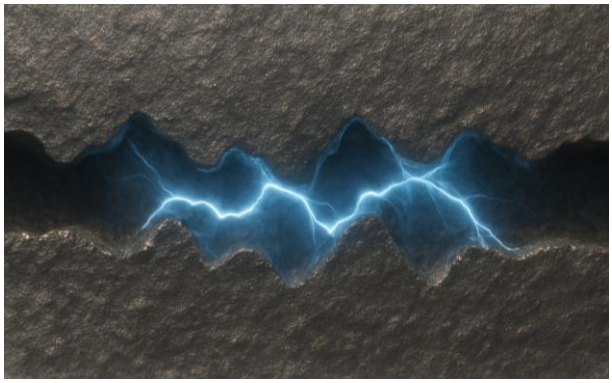

Figure 10. Schematic representation of localized spark discharge due to imperfect electrical contact. The image shows a detailed 2D cross-sectional view of two metallic surfaces in nominal contact, such as a die and a sheet, where surface roughness leads to partial separation and the formation of microscopic air gaps. Upon high-voltage pulse activation, the electric field within these gaps exceeds the dielectric breakdown strength of air, triggering lightning-like spark discharges. These discharges concentrate energy in confined zones, initiating local melting and material damage, ultimately compromising both the sheet and the embedded electrode surfaces.

The difficulty of ensuring consistent electrical contact under industrial forming conditions is well-documented. As noted by Zhang et al., even slight deviations in surface pressure or contact cleanliness

can cause major variations in current path, heat generation, and process stability [25]. In electroplastic forming, most successful implementations to date have relied on external clamping electrodes, which offer better control over contact quality, albeit at the cost of process integration and speed [17], [26]. The present attempt to embed electrodes within forming tools introduces a new level of complexity, where the same surface must satisfy both mechanical and electrical requirements, often in conflict.

One potential mitigation strategy is the use of soft, adaptive contactors, such as spring-loaded graphite brushes or deformable conductive pads, which can conform to surface irregularities and maintain more uniform electrical contact under pressure [27]. Or, to modify the connector shape to tailor it to the sample shape. Such systems have been used successfully in rotary electrical contacts and conductive polymer forming tools [28], and may offer a path forward for integrating PF-TT-EPE into production tooling. However, this would require careful design to prevent contamination, wear, and current localization.

Another challenge lies in the control of pulse energy density relative to the contact area. As this study showed, the same nominal energy density (e.g., 3000 A·ms/mm²) can have dramatically different effects depending on the actual area over which current flows. If that area collapses due to contact instability, local current density skyrockets, leading to discharge. This highlights the need for real-time current monitoring and possibly distributed contact strategies to avoid overload conditions.

In summary, while the concept of PF-TT-EPE remains promising in theory, especially for in-die stress relaxation and springback control, the results of this study underscore the importance of interface engineering. Without reliable, uniform, and conductive contact between die and sheet, the process becomes not only ineffective but potentially destructive. Future work should focus on developing controlled contact solutions, pulse shaping strategies to avoid overvoltage peaks, and perhaps hybrid systems combining electrical and thermal inputs to stabilize the process window.

6. Conclusion

6.1. Main Conclusions

This study introduced and experimentally explored a novel configuration of post-forming electroplastic effect (PF-TT-EPE), aiming to reduce springback by delivering electrical pulses through the thickness of the sheet via embedded electrodes in the forming dies. The following conclusions can be drawn:

- A baseline springback angle of approximately 101.8±0.5° was established for the tested AA5754 alloy using a 90° V-bending tool under mechanically consistent conditions.
- Early attempts at applying a pulse energy density of 3000 A·ms/mm², previously identified as effective in tensile-mode stress relaxation, led to catastrophic spark discharge and irreversible

damage to both the sample and the tool, highlighting the challenges of electrical contact through forming dies.

- The experimental evidence supports the hypothesis that microscale air gaps, resulting from imperfect surface contact and roughness, enable localized dielectric breakdown. This leads to uncontrolled electrical discharge, melting, and material perforation.
- At very low pulse energies (e.g., 274 A·ms/mm²), no electrical degradation occurred, but no significant springback reduction was observed either, suggesting the existence of a critical lower energy threshold required to activate electroplastic mechanisms without inducing material damage.

6.2. Work Boundaries and Limitations

Several limitations constrained the present work:

- Contact instability was the most significant barrier. While mechanical contact could be assured, electrical contact was unreliable, leading to a binary outcome: either no effect or full discharge. This points to a narrow process window that is highly sensitive to surface preparation, pressure uniformity, and interface cleanliness.
- The current setup lacked distributed current control or real-time feedback, making it impossible to manage transient phenomena such as voltage spikes or local overheating.
- The use of a lab-scale pulse generator restricted flexibility in waveform shaping, or fine control of energy delivery, all of which could be critical in refining the interaction between pulse and material.
- The experiments were limited to AA5754 and single-step bending, and do not yet inform whether similar effects can be extended to other alloys, more complex forming geometries, or industrial forming speeds.

6.3. Outlook and Open Research Gaps

While the concept of PF-TT-EPE remains promising for in-die springback reduction, especially from a sustainability and SDG standpoint, this study reveals fundamental technical gaps that must be addressed before practical implementation:

- **Interface Engineering**: New solutions are needed to enable stable and uniform electrical contact under forming pressures. This may include soft conductive contactors, conformal

electrodes, or dynamic pressure modulation to eliminate gaps without compromising tooling integrity.

- **Pulse Delivery Strategies**: The development of smart pulse trains, with tailored voltage ramping, pulse shaping, or energy-dosing mechanisms, may offer more controllable ways to avoid discharge while activating dislocation-based softening mechanisms.
- **Multiphysics Monitoring**: Real-time observation of current distribution, temperature, and acoustic emission could help identify and prevent spark initiation before damage occurs.
- **Modelling and Simulation**: Coupled electromechanical simulations of the PF-TT-EPE system could provide valuable predictive insight into where breakdown is likely and help design safer operating regimes.

In conclusion, this study represents a critical step in identifying both the potential and the fragility of applying electrical pulses through dies for forming enhancement. Future research should focus on interface robustness, energy control, and system integration, all of which are necessary to bridge the gap between laboratory experimentation and industrial implementation.

Acknowledgements

The authors would like to acknowledge the financial support of the Basque Government POSTELEC funded on the Proyectos de investigación program (PI_2017_1_0047) to build the electric pulse generator, and the financial support of Ministerio de Ciencia e Innovación, HEAPLAS «Proyectos de Generación de Conocimiento» PID 2022-139130OA-I00, for the ongoing development.

Declaration of generative AI and AI-assisted technologies in the writing process

During the preparation of this work the author(s) used ChatGPT4o in order to improve the English. After using this tool/service, the author(s) reviewed and edited the content as needed and take(s) full responsibility for the content of the publication.

Data Availability statement (DAS)

Data sets generated during the current study are available from the corresponding author on reasonable request.

Conflict of Interest (COI) statement

The authors declare that they have no conflict of interest.

References

[1] R. A. Antunes and M. C. L. de Oliveira, "Materials selection for hot stamped automotive body parts: An application of the Ashby approach based on the strain hardening exponent and stacking fault energy of materials," *Mater Des*, vol. 63, pp. 247–256, 2014, doi: http://dx.doi.org/10.1016/j.matdes.2014.06.011.

[2] I. Gil, J. Mendiguren, L. Galdos, E. Mugarra, and E. Saenz de Argandoña, "Influence of the pressure dependent coefficient of friction on deep drawing springback predictions," *Tribol Int*, vol. 103, 2016, doi: 10.1016/j.triboint.2016.07.004.

[3] T. Welo, G. Ringen, and J. Ma, "An overview and evaluation of alternative forming processes for complex aluminium products," 2020. doi: 10.1016/j.promfg.2020.05.022.

[4] S. Sulaiman, M. K. A. M. Ariffin, and S. Y. Lai, "Springback Behaviour in Sheet Metal Forming for Automotive Door," *AASRI Procedia*, vol. 3, 2012, doi: 10.1016/j.aasri.2012.11.037.

[5] J. Mendiguren, B. Rolfe, and M. Weiss, "On the definition of an kinematic hardening effect graph for sheet metal forming process simulations," *Int J Mech Sci*, vol. 92, 2015, doi: 10.1016/j.ijmecsci.2014.12.005.

[6] X. A. Yang and F. Ruan, "A die design method for springback compensation based on displacement adjustment," *Int J Mech Sci*, vol. 53, no. 5, 2011, doi: 10.1016/j.ijmecsci.2011.03.002.

[7] A. Rosochowski, "Die compensation procedure to negate die deflection and component springback," *J Mater Process Technol*, vol. 115, no. 2, 2001, doi: 10.1016/S0924-0136(01)00805-6.

[8] R. Lingbeek, J. Huétink, S. Ohnimus, M. Petzoldt, and J. Weiher, "The development of a finite elements based springback compensation tool for sheet metal products," *J Mater Process Technol*, vol. 169, no. 1, 2005, doi: 10.1016/j.jmatprotec.2005.04.027.

[9] H. Hatayama, "The metals industry and the Sustainable Development Goals: The relationship explored based on SDG reporting," *Resour Conserv Recycl*, vol. 178, 2022, doi: 10.1016/j.resconrec.2021.106081.

[10] Y. Yang, L. Zhan, Q. Ma, J. Feng, and X. Li, "Effect of pre-deformation on creep age forming of AA2219 plate: Springback, microstructures and mechanical properties," *J Mater Process Technol*, vol. 229, 2016, doi: 10.1016/j.jmatprotec.2015.10.030.

[11] U. Ulibarri, L. Galdos, E. S. de Argandoña, and J. Mendiguren, "Experimental and numerical simulation investigation on deep drawing process of inconel 718 with and without intermediate annealing thermal treatments," *Applied Sciences (Switzerland)*, vol. 10, no. 2, 2020, doi: 10.3390/app10020581.

[12] Z. Zhang *et al.*, "Springback Reduction by Annealing for Incremental Sheet Forming," in *Procedia Manufacturing*, 2016. doi: 10.1016/j.promfg.2016.08.057.

[13] X. Liu, S. Lan, and J. Ni, "Experimental study of Electro-Plastic Effect on Advanced High Strength Steels," *Materials Science and Engineering: A*, vol. 582, pp. 211–218, Oct. 2013, [Online]. Available: http://www.sciencedirect.com/science/article/pii/S0921509313003912

[14] X. L. Xu, G. G. Zheng, H. D. Wang, and T. Wang, "Research progress on the application of electro-plastic effect in materials processing," *Suxing Gongcheng Xuebao/Journal of Plasticity Engineering*, vol. 24, no. 6, 2017, doi: 10.3969/j.issn.1007-2012.2017.06.001.

[15] S. Adabala, S. Cherukupally, S. Guha, R. D.V, R. K. Verma, and V. R. N, "Importance of machine compliance to quantify electro-plastic effect in electric pulse aided testing: An experimental and numerical study," *J Manuf Process*, vol. 75, 2022, doi: 10.1016/j.jmapro.2021.12.027.

[16] W. Liu *et al.*, "Post-forming, electro-plastic effect internal stress reduction in AA5754 aluminium alloy," *Materials Science and Engineering: A*, vol. 852, p. 143686, Sep. 2022, doi: 10.1016/j.msea.2022.143686.

[17] J. Lozares *et al.*, "AA5754 aluminium alloy springback reduction by post forming electro plastic effect (PFEPE)," *Mechanics of Materials*, vol. 198, p. 105136, Nov. 2024, doi: 10.1016/j.mechmat.2024.105136.

[18] R. Arora, O. Music, and J. M. Allwood, "Understanding the process limits of folding-shearing," *J Mater Process Technol*, vol. 335, p. 118660, Jan. 2025, doi: 10.1016/j.jmatprotec.2024.118660.

[19] F. J. Humphreys and M. Hatherly, *Recrystallization and Related Annealing Phenomena*. 2012. doi: 10.1016/C2009-0-07986-0.

[20] B. Erenturk, M.-H. Park, V. M. Rotello, and K. R. Carter, "Fabrication of air gap dielectrics by nanoimprint lithography," *Microelectron Eng*, vol. 98, pp. 89–96, Oct. 2012, doi: 10.1016/j.mee.2012.03.006.

[21] C. Neusel and G. A. Schneider, "Size-dependence of the dielectric breakdown strength from nano- to millimeter scale," *J Mech Phys Solids*, vol. 63, pp. 201–213, Feb. 2014, doi: 10.1016/j.jmps.2013.09.009.

[22] Y. Deng *et al.*, "Impact of Air Gap Defects on the Electrical and Mechanical Properties of a 320 kV Direct Current Gas Insulated Transmission Line Spacer," *Energies (Basel)*, vol. 16, no. 10, p. 4006, May 2023, doi: 10.3390/en16104006.

[23] A. B. M. A. Asad, M. T. Islam, T. Masaki, M. Rahman, and Y. S. Wong, "Analysis of micro-EDM electric characteristics employing plasma property," *CIRP J Manuf Sci Technol*, vol. 20, pp. 36–50, Jan. 2018, doi: 10.1016/j.cirpj.2017.09.005.

[24] C. M. Dzialo, M. S. Siopis, B. L. Kinsey, and K. J. Weinmann, "Effect of current density and zinc content during electrical-assisted forming of copper alloys," *CIRP Ann Manuf Technol*, vol. 59, no. 1, pp. 299–302, 2010.

[25] C. M. Gheorghita, M. Adam, M. Andrusca, A. Munteanu, and A. Dragomir, "About contact resistance of the electrical equipment," in *2017 International Conference on Modern Power Systems (MPS)*, IEEE, Jun. 2017, pp. 1–4. doi: 10.1109/MPS.2017.7974439.

[26] A. J. Sánchez Egea, H. A. González Rojas, D. J. Celentano, J. A. Travieso-Rodríguez, and J. Llumà I Fuentes, "Electroplasticity-assisted bottom bending process," *J Mater Process Technol*, vol. 214, no. 11, pp. 2261–2267, 2014, doi: 10.1016/j.jmatprotec.2014.04.031.

[27] I. Yasar, A. Canakci, and F. Arslan, "The effect of brush spring pressure on the wear behaviour of copper–graphite brushes with electrical current," *Tribol Int*, vol. 40, no. 9, pp. 1381–1386, Sep. 2007, doi: 10.1016/j.triboint.2007.03.005.

[28] Y. Meng, L. Zhang, G. Xu, and H. Wang, "Direct-current generators based on conductive polymers for self-powered flexible devices," *Sci Rep*, vol. 11, no. 1, p. 20258, Oct. 2021, doi: 10.1038/s41598-021-99447-x.